Rubrique

Identification of self-heating effects on the behaviour of HEMA-EGDMA hydrogels biomaterials using non-linear thermo-mechanical modeling

N. Santatriniaina†, M. Nassajian Moghadam††, D. Pioletti††, L. Rakotomanana†

† Mathematical Research Institute of Rennes
University of Rennes, France.
†† Laboratory of Biomechanical Orthopedics Lausanne
Federal Polytechnic School of Lausanne, Switzerland. nirinasantatriniaina@gmail.com

RÉSUMÉ. Ce papier est dédié à la quantification de la production de chaleur dans l'hydrogel de type HEMA-EGDMA sous chargement dynamique. On s'intéresse à la modélisation du phénomène de self-heating dans les polymères, les hydrogels et les tissus biologiques. On compare les résultats théoriques avec les résultats expérimentaux combinés avec une proposition d'optimisation numérique pour identifier les paramètres influençant le phénomène de self-heating. D'abord, nous nous sommes focalisés sur la modélisation de la loi constitutive de l'hydrogel de type HEMA-EGDMA. Nous avons utilisé la théorie des invariants polynomiaux pour définir la loi constitutive du matériau. Ensuite, nous avons mis en place un modèle théorique en thermomécanique couplée d'un milieu continu classique pour analyser la production de chaleur dans ce matériau. Deux potentiels thermodynamiques ont été proposés et identifiés avec les mesures expérimentales. Une nouvelle forme d'équation du mouvement non-linéaire et couplée a été obtenue. Enfin, une méthode numérique des équations thermo-mécaniques pour les modèles a été utilisée. Cette étape nous a permis, entre autres, de résoudre ce système couplé. La méthode numérique est basée sur la méthode des éléments finis.

ABSTRACT. This paper is dedicated to the quantification of the heat production in the HEMA-EGDMA hydrogel under dynamic loading. We focus on modeling of the self-heating phenomenon in polymers, hydrogels and biological tissues. We compare the theoretical and experimental results combined with numerical optimization proposal to identify the influencing parameters on the self-heating phenomenon. We develop constitutive law of the HEMA-EGDMA hydrogel, focusing on the heat effects in this material. We set up a theoretical model of coupled thermo-mechanical classic continuum for a better understanding of the heat production in this media. We use polynomial invariants theory to define the constitutive law of the media. Two thermodynamic potentials are proposed and are identified with the experimental measurements. New form of non-linear and coupled governing equations were obtained. Numerical methods were used to solve thermo-mechanical formalism for the model. Then, this step allows us, among other things, to propose an appropriate numerical methods to solve this system. The numerical methods is based on the finite element methods.

MOTS-CLÉS : Hydrogel, self-heating, thermomécanique, méthodes numériques, EDPs.

KEYWORDS : Hydrogel, self-heating, thermomechanics, numerical methods, PDEs.

1. Introduction

Hydrogels have been widely employed in biomedical areas [1], [2], [3]. The thermomechanical response of these materials depends strongly on temperature, cross-link density and frequency if the hydrogel is under cyclic loading [4]. Particular hydrogel possessing high dissipation properties may induce a heat production under cyclic loading [5]. Due to the heat production, an increase of the local temperature can be observed in the material, a phenomenon also known as self-heating [4], [5]. In turn, the increase in temperature has an effect on its properties and on the thermomechanical behavior [5], [6], [7]. Modeling and simulation methods are one of the strong characterization methods of the physical phenomena in this kind of material [8], [9]. When the sample is simultaneously subjected to mechanical and thermal loads, we need to develop experimental tool and coupled formulation to investigate and to measure simultaneously the mechanical response and the heat production in the sample [9], [10], [11]. The goal of this work is to identify a constitutive law based on generalized standard materials in correlation with the experimental measurements. Numerical methods for a coupled partial differential equation with dynamic boundary conditions are developed with the conservation laws [12], [13], [14]. Nonlinear constitutive law for viscoelastic material without heat effect has been established by Pioletti, Rakotomanana *et al.* for biological tissues in large deformation [9]. The present work extends this model to nonlinear constitutive law for thermo-viscoelastic model with heat effect in the particular case of matrix HEMA-EGDMA hydrogel. In this work, a general continuum thermomechanical framework describing the effect is adapted to the description of the self-heating phenomenon. Numerical studies are then carried out to examine the ability of the model to predict the heat production and to define the nature of the coupling as well as to evaluate the influence of the main parameters such as cross-link density and frequency of loading. In parallel, microcalorimetric experimental measurements are performed to quantify the heat production and the mechanical response in the HEMA-EGDMA hydrogel sample.

2. Microcalorimetric test

In order to characterize the heat production in the hydrogel samples, an adiabatic deformation microcalorimeter is used [4]. The hydrogel sample consists of cylindrical samples 5 mm of diameter and 8 mm of height are subjected to cyclic mechanical load at various frequencies $f = 0.5, ..., 1Hz$. For the mechanical boundary conditions, on the top of the cylinder we apply the cyclic load, while the bottom is fixed. For the thermal boundary condition, we have an adiabatic condition (non inward and outward flux). The initial conditions are : initial stress null and initial temperature θ_0. The heat production is measured with a specific sensor inserted within the sample and the data acquisition is directly obtained with a computer. For a more detailed description, the reader is reffered to [4]. The displacement is prescibed on the top of the sample to 20% of the sample height. The sample loading is done in three parts including preload, cyclic loading and relaxation. And the bottom of the sample is "fixed". We chose 30 s of preload, 5 mn cyclic loading and 5 mn relaxation. For the sample we use the composition is given by : HEMA+40%w+ϕ% EGDMA with 8.93 mm diameter, 5.33 mm of height, 40% of water, 6% and 8% of crosslink density.

3. Mathematical settings

The self-heating phenomena are governed by a nonlinear-coupled partial differential equation system deduced from two conservation equations of classical continuum thermomechanics. We assume the postulate of the existence of two thermodynamic potentials the strain energy function and the dissipation potential defined per unit of the reference volume. The model is obtained by constructing with the free energy method, new non-negative convex energy functions given by the equation (1). For physical and mathematical considerations, convexity/polyconvexity of the strain energy and dissipation functions are an essential point since the common methods in computer simulation depend on gradient methods.

$$\psi(\mathbf{E},\theta) = \frac{\lambda}{2}\mathrm{tr}^2\mathbf{E} + \mu\mathrm{tr}\mathbf{E}^2 - (3\lambda+2\mu)\alpha\mathrm{tr}\mathbf{E}(\theta-\theta_0) - \frac{c_v}{2\theta_0}(\theta-\theta_0)^2$$
$$\chi(\dot{\mathbf{E}},\nabla\theta) = \frac{\lambda'}{2}\mathrm{tr}^2\dot{\mathbf{E}} + \mu'\mathrm{tr}\dot{\mathbf{E}}^2 + \frac{\kappa}{2}||\nabla\theta||^2 \tag{1}$$

where λ, μ, α, c_v, λ', μ' and κ are respectively the Lamé constants, the thermal expansion coefficient, specific heat capacity coefficient, viscosity coefficient and heat conduction coefficient. The reference temperature is denoted by θ_0. Parameters α, c_v and κ are considered as constants.

Hypothesis 3.1. *For the thermodynamic potentials given by the relations* (1)*, the Lamé's constants λ, μ are known for the hydrogel HEMA-EGDMA, the specific heat capacity coefficient is estimated by microcalorimetric test. The remaining constant are unknowns ($\alpha[1/K]$, $\lambda'[MPa.s]$, $\mu'[MPa.s]$ and $\kappa[W/(m.K)]$). We assume the following mechanical properties for the sample :*

Samples	E[MPa]	ν	$\lambda[MPa]$	$\mu[MPa]$	$c_v[J/(kg.K)]$
Sample 1	10-30	0.45	3.10-9.3	0.34-1.02	2900-3200
Sample 2	20-50	0.40	2.86-7.15	0.71-1.78	2900-3200

The balance of linear momentum and the energy conservation allow us to express the governing equations of the hydrogel sample and can be formulated as :

$$\begin{cases} \mathbf{DivFS^e} + \mathbf{DivFS^v} + \rho\mathbf{B} = \rho\dfrac{\partial^2\mathbf{u}}{\partial t^2} & \text{in } (\mathcal{B}\times[0,T]) \\ \rho\dot{e} = (\mathbf{S^e}+\mathbf{S^v}) : \dot{\mathbf{E}} - \mathbf{DivQ} + \rho r & \text{in } (\mathcal{B}\times[0,T]) \end{cases} \tag{2}$$

where $\mathbf{S^e}(\mathbf{E},\theta) = \rho\partial\psi/\partial\mathbf{E}(\mathbf{E},\theta)$ and $\mathbf{S^v}(\dot{\mathbf{E}},\nabla\theta) = \partial\chi/\partial\dot{\mathbf{E}}(\dot{\mathbf{E}},\nabla\theta)$ are the elastic and viscous parts of the second Piola-Kirchhoff stress tensor $\mathbf{Q}/\theta = -\partial\chi/\partial\nabla\theta(\dot{\mathbf{E}},\nabla\theta)$ is the heat flux, $e = \psi(\mathbf{E},\theta) + s\theta$ the internal energy, $s = -\partial\psi/\partial\theta(\mathbf{E},\theta)$ the entropy density and $\mathbf{E} = \nabla\mathbf{u} + \nabla^{\mathbf{T}}\mathbf{u} + \nabla\mathbf{u}\nabla^{\mathbf{T}}\mathbf{u}/2$ is the Green-Lagrange strain tensor.

Equations of the three-dimensional continuum, developed avove, define the initial boundary value problem of thermomechanics. In detail, these were the description of deformation in the context of kinematics, the formulation of the force equilibrium based on kinetic considerations, the constitutive equation as well as the initial and boundary conditions. We assume the following mechanical boundary conditions which include three parts, preloading, cyclic loading and relaxation ($\mathbf{S}^t\mathbf{DN}$).

$$\begin{cases} \mathbf{u}\cdot\mathbf{n} = -\begin{cases} u_p\left(\dfrac{t}{\tau}\right) & \text{if } t < t_p \\ u_p\left(\dfrac{t_p}{\tau}\right) + \mathbf{u}_0\cos(2\pi f t) & \text{if } t_p \le t \le t_c \end{cases} & \text{on } (\Gamma_t \times [0,T]) \\ \mathbf{P}\cdot\mathbf{n} = \mathbf{0} & \text{if } t > t_c \quad \text{on } (\Gamma_t \times [0,T]) \\ \mathbf{P}\cdot\mathbf{n} = \mathbf{0} & \text{on } (\Gamma_l \times [0,T]) \\ \mathbf{u}\cdot\mathbf{n} = u_0 & \text{on } (\Gamma_u \times [0,T]) \\ \mathbf{P} = \mathbf{F}(\mathbf{S^e} + \mathbf{S^v}) \text{ in } (\mathcal{B}\times[0,T]) & \\ \textbf{I.C } \mathbf{u}(t=0,\cdot) := 0,\ \mathbf{P}(t=0,\cdot) := \mathbf{0} & \text{in } (\mathcal{B}\times\{0\}) \end{cases} \tag{3}$$

where $\tau \in \mathcal{R}_+$ is a time constant. $u_p \in \mathcal{R}$ denotes the prescribed displacement during the preloading and the relaxation. $u_0 \in \mathcal{R}$ denotes the prescribed displacement during the cyclic loading. We consider two time characteristics $t_p \in \mathcal{R}_+$ the preloading time and $t_c \in \mathcal{R}_+$ the time during which the cyclic load is applied. Experimentally, we apply the preload as a ramp form during the preload time t_p. Then we apply the mechanical cyclic loading during the load time t_c. Finally, after $t_c + t_p$, the discharge and relaxation time are beginning for a new t_p. For the heat boundary condition, we use the same continuous

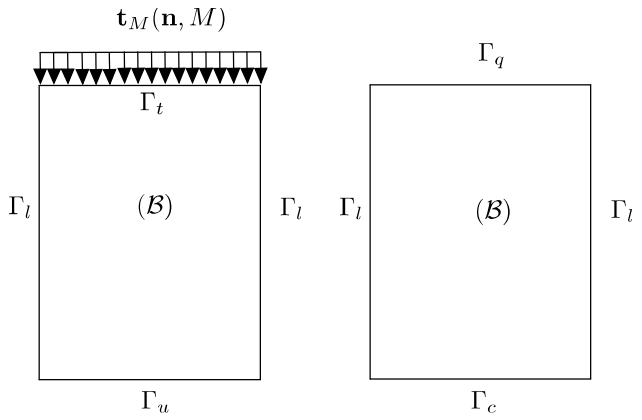

Figure 1. *Boundary conditions : mechanical boundary conditions (left), heat transfer boundary conditions (right).*

media $\mathcal{B} \in \mathcal{R}^d$ with the $V^{\mathcal{B}}$ the volume. The boundary of $\mathcal{B}$ is $\partial\mathcal{B} = \Gamma_q \cup \Gamma_l \cup \Gamma_c$ with the surface $S^{\mathcal{B}}$. For each time $t \in \mathcal{R}_+$ this volume is under heat production density ρr, a heat flux q_0 on one parts of the boundary of $\mathcal{B}$ and with a prescribed temperature θ_0 on other parts of the boundary of $\mathcal{B}$. The heat boundary can written as :

$$\begin{cases} \mathbf{Q}\cdot\mathbf{n} = q_0 & \text{on } (\Gamma_q \times [0,T]) \\ \mathbf{Q}\cdot\mathbf{n} = 0 & \text{on } (\Gamma_l \times [0,T]) \\ \mathbf{Q}\cdot\mathbf{n} = k_c(\theta - \theta_\infty) & \text{on } (\Gamma_c \times [0,T]) \\ \textbf{I.C } \theta(t=0,\cdot) := \theta_{ref} & \text{in } (\mathcal{B}\times\{0\}) \end{cases} \tag{4}$$

in which, q_0 is the prescribed heat flux on $(\Gamma_q \times [0,T])$, k_c denotes the convection coefficient and θ_0 is the prescribed temperature, θ_{ref} is the initial local temperature of the sample and θ_0 is the thermodynamic temperature.

By using the definition of the potential ψ and χ in the equation (1), the elastic and viscous parts of the second Piola-Kirchhoff hold :

$$\mathbf{S^e} = \lambda \mathrm{tr}(\mathbf{E})\mathbf{I} + 2\mu\mathbf{E} - (3\lambda + 2\mu)\alpha(\theta - \theta_0)\mathbf{I}; \quad \mathbf{S^v} = \lambda' \mathrm{tr}(\dot{\mathbf{E}})\mathbf{I} + 2\mu'\dot{\mathbf{E}} \tag{5}$$

In order to identify the numerical parameters of the self-heating model with the experimental measurements and for the correlation study, we compute the Cauchy stress tensor in the current configuration. For this purpose, we use the classical formulation with the deformation gradient. Then, the elastic part and the viscous part of the Cauchy stress tensor are given successively by :

$$\begin{aligned} \sigma^{\mathbf{e}} = \frac{\lambda}{J}\mathrm{tr}(\mathbf{E})\mathbf{F}\mathbf{I}\mathbf{F}^{\mathbf{T}} + 2\frac{\mu}{J}\mathbf{F}\mathbf{E}\mathbf{F}^{\mathbf{T}} - (3\lambda + 2\mu)\frac{\alpha}{J}(\theta - \theta_0)\mathbf{F}\mathbf{I}\mathbf{F}^{\mathbf{T}} \\ \sigma^{\mathbf{v}} = \frac{\lambda'}{J}\mathrm{tr}(\dot{\mathbf{E}})\mathbf{F}\mathbf{I}\mathbf{F}^{\mathbf{T}} + 2\frac{\mu'}{J}\mathbf{F}\dot{\mathbf{E}}\mathbf{F}^{\mathbf{T}} \end{aligned} \tag{6}$$

Starting from the expression of the heat flux $\mathbf{Q} = -\kappa\theta\nabla\theta$ in $(\mathcal{B} \times [0, T])$, by using the divergence theorem and rearranging the terms in the heat equation, the governing equation (2) can be written as :

$$\begin{cases} \mathbf{Div}\left[\rho(\lambda \mathrm{tr}(\mathbf{E})\mathbf{F}\mathbf{I} + 2\mu\mathbf{F}\mathbf{E}) - (3\lambda + 2\mu)\alpha(\theta - \theta_0)\mathbf{F}\mathbf{I}\right] + \mathbf{Div}\left[\lambda' \mathrm{tr}(\dot{\mathbf{E}})\mathbf{F}\mathbf{I} + 2\mu'\mathbf{F}\dot{\mathbf{E}}\right] \\ +\rho\mathbf{b} = \rho\dfrac{\partial^2\mathbf{u}}{\partial t^2} \text{ in } (\mathcal{B} \times [0, T]) \\ \rho\dfrac{c_v}{\theta_0}\dfrac{\partial\theta}{\partial t}\theta = (3\lambda + 2\mu)\alpha\theta \mathrm{tr}\dot{\mathbf{E}} + \lambda' \mathrm{tr}^2\dot{\mathbf{E}} + 2\mu' \mathrm{tr}\dot{\mathbf{E}}^2 - \kappa\theta\Delta\theta + \kappa||\nabla\theta||^2 + \rho r \\ \textbf{B.C} \text{ and } \textbf{I.C} \text{ (Cf. eq.(3) and (4))} \end{cases} \tag{7}$$

We assume two cases :

– Case 1 : **Local self-heating model** $\kappa \equiv 0$, $\mathbf{Q} \equiv 0$ For the hydrogel HEMA-EGDMA, the heat conductivity coefficient is very small ($\kappa \equiv 0$), then the heat flux by conduction in the sample is neglected ($\mathbf{Q} \equiv 0$). Analogously, the change in internal energy caused by the sources of heat is local vanishes and there is no heat diffusion in the media.

Hypothesis 3.2 (Local self-heating model). *We assume for this case that we have a local heat production. The internal heat production is not function of the space but just function of time $\theta := \theta(t)$. In this case, the quantity $\mathbf{Div}\left[(3\lambda + 2\mu)\alpha(\theta - \theta_0)\mathbf{F}\mathbf{I}\right] \equiv 0$ (effect of the temperature change on stress) in the governing equation* (7)*. In fact, we have the effect of the velocity on the internal heat production.*

For the second approximation we assume that, for the hydrogel HEMA-EGDMA, the heat conductivity coefficient of the sample is significant ($\kappa \neq 0$), then the heat flux by conduction in the sample is also significant ($\mathbf{Q} \neq 0$). Indeed, the change in internal energy is caused by the sources of heat and the deformation.

– Case 2 : $\kappa \neq 0$,

Hypothesis 3.3 (Total self-heating model). *In this case, we assume that the total heat is function of the space, the gradient of temperature and displacement. In fact, the heat conductivity is not neglected, then, the internal heat production is function of the space and time $\theta := \theta(x, t)$. In this case, the quantity $\mathbf{Div}\left[(3\lambda + 2\mu)\alpha(\theta - \theta_0)\mathbf{F}\mathbf{I}\right] \neq 0$ (effect of the temperature on stress) in the governing equation* (7)*. In fact, we have the two coupling terms : the effect of the velocity on the internal heat production and the effect of the temperature change on the stress.*

The character of the initial boundary value problem of structural mechanics depends on the types of structure and loading that have to be described, which, on the other hand, decisively affect the modeling of the load-carrying behavior. In the previous sections, the essential modeling aspects were already discussed on geometrical and material levels. In summary, the modeling can be categorized, in essence, according to the aspects of geometrical linearity or non-linearity, material linearity or non-linearity, and time-dependence or time-independence. The various approximation levels differ significantly in the complexity of the numerical solution of the underlying physical problem. The correlation between the simplification of the physical problem and the complexity of the numerical solution is illustrated in this work. Furthermore, the dynamic or static formulation of the problem is decisive for the effort expanded on the numerical solution.

We assume linearity of the temperature and the displacement. For physical consideration, the sample dimension is small for the hydrogel HEMA-EGDMA, we therefore assume that the heat production in the sample is local.

Hypothesis 3.4 (**Linearity in temperature**). *We assume small variation of the temperature distribution in the sample the prescribed cyclic displacement. The temperature $\theta \in \mathcal{R}_+$ is expessed as a reference temperature $\theta_0 \in \mathcal{R}_+$ plus the perturbation $\delta\theta \in \mathcal{R}_+$. We have : $\theta = \theta_0 + \delta\theta$ and $\dot{\theta} = \delta\dot{\theta}$.*

– Case 1 : **Local self-heating model** $\kappa \equiv 0$, $\mathbf{Q} \equiv 0$, Cf. hypothesis 3.2
The governing equation can be written as follows :

$$\begin{cases} \mathbf{Div}\left[\rho(\lambda \mathrm{tr}(\mathbf{E})\mathbf{FI} + 2\mu\mathbf{FE}) - (3\lambda+2\mu)\alpha\delta\theta\mathbf{FI}\right] + \mathbf{Div}\left[\lambda' \mathrm{tr}\dot{\mathbf{E}}\mathbf{FI} + 2\mu'\mathbf{F}\dot{\mathbf{E}}\right] \\ +\rho\mathbf{B} = \rho\dfrac{\partial^2\mathbf{u}}{\partial t^2} \text{ in } (\mathcal{B}\times[0,T]) \\ \rho c_v \dfrac{\partial\delta\theta}{\partial t} = (3\lambda+2\mu)\alpha(\theta_0+\delta\theta)\mathrm{tr}\dot{\mathbf{E}} + \lambda'\mathrm{tr}^2\dot{\mathbf{E}} + 2\mu'\mathrm{tr}\dot{\mathbf{E}}^2 + \rho r \text{ in } (\mathcal{B}\times[0,T]) \\ \textbf{B.C} \text{ and } \textbf{I.C} \text{ (Cf. eq.(3) and (4))} \end{cases} \tag{8}$$

– Case 2 : **Total self-heating model** $\kappa \neq 0$, $\mathbf{Q} \neq 0$, Cf. hypothesis 3.3.
The governing equation can be written as follows :

$$\begin{cases} \mathbf{Div}\left[\rho(\lambda \mathrm{tr}(\mathbf{E})\mathbf{FI} + 2\mu\mathbf{FE}) - (3\lambda+2\mu)\alpha\delta\theta\mathbf{FI}\right] + \mathbf{Div}\left[\lambda' \mathrm{tr}(\dot{\mathbf{E}})\mathbf{FI} + 2\mu'\mathbf{F}\dot{\mathbf{E}}\right] \\ +\rho\mathbf{B} = \rho\dfrac{\partial^2\mathbf{u}}{\partial t^2} \text{ in } (\mathcal{B}\times[0,T]) \\ \rho c_v \dfrac{\partial\delta\theta}{\partial t} = (3\lambda+2\mu)\alpha(\theta_0+\delta\theta)\mathrm{tr}\dot{\mathbf{E}} + \lambda'\mathrm{tr}^2\dot{\mathbf{E}} + 2\mu'\mathrm{tr}\dot{\mathbf{E}}^2 - \kappa\theta_0\Delta\delta\theta + \rho\mathbf{R} \\ \text{in } (\mathcal{B}\times[0,T]) \\ \textbf{B.C} \text{ and } \textbf{I.C} \text{ (Cf. eq.(3) and (4))} \end{cases} \tag{9}$$

In order to show the solution of the problem with the applicability of the thermoviscoelastic model as defined in the equation (9), we firstly assume one and two dimensional problem.

4. 2D and 1D approaches

As preliminary steps, it is important to recall the two and monodimensional formulation. The thermomechanical formulation will help us to understand each term appearing

in the equation (9). We assume one-dimensional compression. For the deformation analysis of two-dimensional continua, the plane stress and the plane strain states are of interest. The plane strain state is mostly used in cases where the dimension in one direction is very large with the loading in this direction remaining unchanged. The derivation of these equations can be found in the following sections.

Hypothesis 4.1 (Small strain assumption)**.** *As a first approximation the essential components of the description are small, linear elastic deformations*

We used the dimensionless form of the govering equation. For this purpose, we introduce new variables as defined in the equation (21) :

$$\hat{x} = \frac{x}{\ell}; \quad \hat{u} = \frac{u}{u_0}; \quad \hat{\dot{u}} = \frac{\dot{u}}{\dot{u}_0}; \quad \hat{t} = \frac{t}{t_0}; \quad \delta\hat{\theta} = \frac{\delta\theta}{\theta_0}. \tag{10}$$

The governing equation with the initial and the boundary conditions, and keeping the notation u but not $\hat{u}$ can be written in the following form :

$$\begin{cases} \dfrac{A}{C}\left(\dfrac{\partial^2 u}{\partial x^2}\right) + \dfrac{G}{C}\left(\dfrac{\partial \delta\theta}{\partial x}\right) + \dfrac{B}{C}\left(\dfrac{\partial^2 \dot{u}}{\partial x^2}\right) + \rho\bar{b} = \dfrac{\partial^2 u}{\partial t^2} \quad \text{in } (\mathcal{B}\times[0,T]) \\ \dfrac{\partial \delta\theta}{\partial t} = \dfrac{D}{F}(\theta_0+\delta\theta)\left(\dfrac{\partial \dot{u}}{\partial x}\right) + \dfrac{E}{F}\left(\dfrac{\partial^2 \dot{u}}{\partial x^2}\right) + \dfrac{H}{F}\dfrac{\partial^2 \theta\theta}{\partial x^2} + \rho\bar{R} \quad \text{in } (\mathcal{B}\times[0,T]) \\ \delta\theta(x,0) = \theta_{ref}; \quad \left(-\kappa\dfrac{\partial \delta\theta}{\partial x}\right)_{x=0} = 0; \quad \left(-\kappa\dfrac{\partial \delta\theta}{\partial x}\right)_{x=\ell} = 0; \quad u(0,t) = 0 \\ u(\ell,t) = u_\ell \sin(\omega t); \quad u(x,0) = 0; \quad \dot{u}(x,0) = 0 \end{cases} \tag{11}$$

In which,

$$A = \rho\frac{(\lambda+2\mu)}{\ell^2}u_0^2; \quad B = \frac{(\lambda'+2\mu')}{\ell^2}\dot{u}_0^2; \quad C = \rho\frac{u_0}{t_0^2}; \quad F = \rho c\frac{\theta_0}{t_0}; \tag{12}$$

$$D = \frac{(3\lambda+2\mu)\alpha\theta_0}{\ell}\dot{u}_0; \quad E = \frac{(\lambda'+2\mu')}{\ell^2}\dot{u}_0^2; \quad G = \frac{(3\lambda+2\mu)\rho\alpha}{\ell}\theta_0; \quad H = \frac{\kappa\theta_0^2}{\ell^2}. \tag{13}$$

– Case 1 : **Local self-heating model**, $\kappa \equiv 0$, $\frac{G}{C}\frac{\partial\theta}{\partial x} \equiv 0$, $\frac{H}{F}\frac{\partial^2\theta}{\partial x^2} \equiv 0$, Cf. hypothesis 3.3.

For the first approximation, we assume that the heat source $\rho r = 0$ and the body force $\rho\bar{b} = 0$, then, we introduce $K_1 := \frac{A}{C}$, $K_2 := \frac{B}{C}$, $K_3 := \frac{D}{F}$, $K_4 := \frac{E}{F}$. For the first equation, we use the variable (space-time) separation $u(x,t) = \phi(x)T(t)$ in the first equation, for a physic solution we have $\ddot{T}(t) + K_2k^2\dot{T}(t) + K_1k^2T(t) = 0$. The characteristic equation is given by $r^2 + K_2k^2r + K_1k^2 = 0$, the discriminant is $\Delta = K_2^2k^4 - 4K_1k^2$. We define a critical damping for $\Delta = 0$, $K_2^c = 2\frac{\sqrt{K_1}}{k}$, the damping coefficient is defined as $\zeta := \frac{K_1}{K_2^c} = \frac{K_2k}{2\sqrt{K_1}}$. We denote by $\Omega_0 = K_1k^2$, we have $\ddot{T}(t) + 2\zeta k\Omega_0\dot{T}(t) + \Omega_0^2T(t) = 0$ The characteristics equation is given by $s^2 + 2\zeta\Omega_0 s + \Omega_0^2 = 0$, the discriminant is $\Delta_s = 4\Omega_0^2\left(\zeta^2 - 1\right)$. For the solution, we assume that $T(0) = T_0$, $\dot{T}(0) = 0$ and consider following three cases :

1) **Critical damping** $\zeta = 1$, $\Delta_s = 0$, $s = -\Omega_0$ The solution is $T(t) = ae^{st} = ae^{-\Omega_0 t}$, the expression $bte^{-\Omega_0 t}$ also satisfies the differential equation. We have $T(t) = (a+bt)e^{st}$, in which $a = T_0$ and $b = T_0\omega_0$, In this case we have

$$T(t) = T_0(1 + \Omega_0 t)e^{-\Omega_0 t}$$

$$u(x,t) = T_0 \sum_{n=1}^{+\infty} u_\ell \frac{\sin(\omega_n t)}{\sin(k\ell)} \sin(k_n x)(1 + \Omega_0 t) e^{-\Omega_0 t}$$

$$\delta\theta(t;x) = \sum_{n=1}^{+\infty} \frac{K_4}{K_3} k \tan(k_n x)$$

$$+ \sum_{n=1}^{+\infty} \exp\left(- \frac{e^{-\Omega_0 t} k \cos(k_n x) \sin(\omega_n t) K_3 T_0 u_\ell \, (1 + \Omega \, t_0)}{\sin(k\ell)} \right) \left(\theta_{ref} - \frac{K_4}{K_3} k \tan(k_n x) \right)$$

$$S_{33} = \sum_{n=1}^{+\infty} \frac{T_0 u_\ell k\ell}{\sin(k\ell)} e^{-\Omega_0 t} \cos(k_n x) \left[\omega \cos(\omega_n t) K_2 \, (1 + \Omega_0 t) \right]$$

$$\sum_{n=1}^{+\infty} \frac{T_0 u_\ell k\ell}{\sin(k\ell)} e^{-\Omega_0 t} \cos(k_n x) \left[+ \sin(\omega_n t) \left(-K_2 \Omega_0^2 t + K_1 \, (1 + \Omega_0 t) \right) \right]$$

2) **Sub-critical damping** $\zeta < 1$, $\Delta_s < 0$

$$s_1 = -\Omega_0 \left(\zeta + j\sqrt{1-\zeta^2} \right), \qquad s_2 = -\Omega_0 \left(\zeta - j\sqrt{1-\zeta^2} \right), \qquad j^2 = -1 \tag{14}$$

We denote by $\Omega = \Omega_0 \sqrt{1-\zeta^2}$ the solution can be written as :

$$T(t) = \frac{T_0}{2} \left[\left(1 + \frac{j\zeta\Omega_0}{\Omega} \right) e^{-(\Omega_0 \zeta + j\Omega)t} + \left(1 - \frac{j\zeta\Omega_0}{\Omega} \right) e^{-(\Omega_0 \zeta - j\Omega)t} \right]$$

$$T(t) = \frac{T_0}{2} e^{-\Omega_0 \zeta t} \left[\left(1 + \frac{j\zeta\Omega_0}{\Omega} \right) e^{-j\Omega t} + \left(1 - \frac{j\zeta\Omega_0}{\Omega} \right) e^{j\Omega t} \right] \tag{15}$$

Using the transformation of $e^{-j\Omega t}$ and $e^{j\Omega t}$, we have

$$T(t) = T_0 e^{-\Omega_0 \zeta t} \left[\cos(\Omega t) + \frac{\Omega_0 \zeta}{\Omega} \sin(\Omega t) \right]$$

$$u(x,t) = T_0 \sum_{n=1}^{+\infty} u_\ell \frac{\sin(\omega_n t)}{\sin(k\ell)} \sin(k_n x) e^{-\Omega_0 \zeta t} \left[\cos(\Omega t) + \frac{\Omega_0 \zeta}{\Omega} \sin(\Omega t) \right]$$

$$\delta\theta(t;x) = \sum_{n=1}^{+\infty} \frac{K_4}{K_3} k \tan(k_n x)$$

$$+ \sum_{n=1}^{+\infty} \exp\left(- \frac{e^{-\zeta\Omega_0 t} k \cos(k_n x) \sin(\omega_n t) K_3 T_0 u_\ell \, (\Omega \cos(\Omega t) + \zeta \sin(\Omega t) \Omega_0)}{\sin(k\ell)\Omega} \right)$$

$$\left(\theta_{ref} - \frac{K_4}{K_3} k \tan(kx) \right)$$

$$S_{33} = \sum_{n=1}^{+\infty} \frac{T_0 u_\ell k\ell}{\sin(k_n x)\Omega} e^{-\zeta\Omega_0 t} \cos(k_n x) \left[\omega \cos(\omega_n t) K_2 \, (\Omega \cos(\Omega t) + \zeta \sin(\Omega t) \Omega_0) \right]$$

$$+ \sum_{n=1}^{+\infty} \frac{T_0 u_\ell k\ell}{\sin(k_n x)\Omega} e^{-\zeta\Omega_0 t} \cos(k_n x) \left[\sin(\omega_n t) \left(K_1 \, (\Omega \cos(\Omega t) + \zeta \sin(\Omega t) \Omega_0) \right) \right]$$

$$+ \sum_{n=1}^{+\infty} \frac{T_0 u_\ell k\ell}{\sin(k_n x)\Omega} e^{-\zeta\Omega_0 t} \cos(kx) \left[\sin(\omega_n t) \left(-\sin(\Omega t) K_2 \left(\Omega^2 + \zeta^2 \Omega_0^2 \right) \right) \right]$$

3) **Super-critical damping** $\zeta > 1$, $\Delta_s > 0$

$$s_1 = -\Omega_0 \left(\zeta + \sqrt{\zeta^2 - 1} \right), \qquad s_2 = -\Omega_0 \left(\zeta - \sqrt{\zeta^2 - 1} \right) \tag{16}$$

The solution is

$$T(t) = \frac{T_0}{2} e^{-\zeta\Omega_0 t}\left[(1-Y)\, e^{-\Omega_0\sqrt{\zeta^2-1}t} + (1+Y)\, e^{\Omega_0\sqrt{\zeta^2-1}t}\right]$$

$$u(x,t) = \frac{T_0}{2}\sum_{n=1}^{+\infty} u_\ell \frac{\sin(\omega_n t)}{\sin(k\ell)}\sin(k_n x) e^{-\zeta\Omega_0 t}\left[(1-Y)\, e^{-\Omega_0\sqrt{\zeta^2-1}t}\right]$$

$$\frac{T_0}{2}\sum_{n=1}^{+\infty} u_\ell \frac{\sin(\omega_n t)}{\sin(k\ell)}\sin(k_n x) e^{-\zeta\Omega_0 t}\left[+(1+Y)\, e^{\Omega_0\sqrt{\zeta^2-1}t}\right]$$

$$\delta\theta(t;x) = \sum_{n=1}^{+\infty}\frac{K_4}{K_3} k\tan(k_n x)$$

$$+\sum_{n=1}^{+\infty}\exp\left[-\frac{2e^{-\zeta\Omega_0 t}k\cos(k_n x)\sin(\omega_n t)\zeta\sinh\left(Y_s\Omega_0 t\right)K_3 T_0 u_\ell}{\sin(k\ell)\sqrt{\zeta^2-1}}\right]\left(\theta_{ref} - \frac{K_4}{K_3}k\tan(k_n x)\right)$$

$$+\sum_{n=1}^{+\infty}\exp\left[-\frac{2e^{-\zeta\Omega_0 t}k\cos(k_n x)\sin(\omega t)Y_s\cosh\left(Y_s\Omega_0 t\right)K_3 T_0 u_\ell}{\sin(k\ell)Y_s}\right]\left(\theta_{ref} - \frac{K_4}{K_3}k\tan(k_n x)\right)$$

$$S_{33} = \sum_{n=1}^{+\infty}\frac{T_0 u_\ell k\ell\cos(k_n x)}{\sin(kl)Y_s} e^{-(\zeta+Y_s)\Omega_0 t}\left\{\left[\left(-1+e^{2Y_s\Omega_0 t}\right)\zeta + \left(1+e^{2Y_s\Omega_0 t}\right)Y_s\right]\right.$$

$$\sin(\omega_n t)K_1 + K_2\left[\left(-1+e^{2Y_s\Omega_0 t}\right)\zeta + \left(1+e^{2Y_s\Omega_0 t}\right)Y_s\right]\omega\cos(\omega_n t)$$

$$\left.-K_2\left(-1+e^{2Y_s\Omega_0 t}\right)\sin(\omega_n t)\Omega_0\right\}$$

In which $Y = \frac{\zeta}{\sqrt{\zeta^2-1}}$ and $Y_s = \sqrt{\zeta^2-1}$.

– Case 2 : **Total self-heating model**, $\kappa \neq 0$, $\frac{G}{C}\left(\frac{\partial\theta}{\partial x}\right) \neq 0$, $\frac{H}{F}\theta\frac{\partial^2\theta}{\partial x^2} \neq 0$, Cf. hypothesis 3.3.

Remark 4.1. *The local behavior of a thermoviscoelastic body for one dimensional problem was totally described in the previous section by means of the initial boundary value problem. Generally, the solution of this differential equation is not analytically explicit. Therefore, approximation methods, in particular the Finite Element Method, are used in order to find an approximate solution. This method does not solve the strong form of the differential equation. It merely solves its integral over the domain, the so-called weak form of the differential equation. This weak formulation forms the basic prerequisite for the application of approximation methods.*

5. Identification of the model parameters

For a given thermodynamic potential, the main problem after the formulation is to calculate or measure the physical constants in the model. If the physical constants can be identified with the experimental measurement, it is appropriate to determine these constants by using classical identification procedures. In the opposite case, we need to identify these constants by using analytical/numerical approaches. For that, we use the one dimension analytical description in order to identify the physical constant in the model.

5.1. Cost functions

According to the classical method of optimization, the identification method of physical constant in the model of self-heating (thermoviscoelasticity) can be expressed using complex parameters. The parameters to be identified are α, λ', μ' and κ

Definition 5.1 (Cost functions)**.** *The cost function for the self-heating model is given by the following equation and we have to minimize the following coupled cost function :*

$$\mathbf{x} = \inf_{\alpha\in\mathcal{R}_+}\inf_{\lambda'\in\mathcal{R}_+}\inf_{\mu'\in\mathcal{R}_+}\inf_{\kappa\in\mathcal{R}_+}\left\{\begin{array}{l} f\left(\left(\frac{2}{J}\mathbf{F}\mathbf{S}\mathbf{F}^{\mathbf{T}}\right)^{comp}(\alpha,\lambda',\mu') - \sigma^{obse}\right) \\ g\left(\delta\theta^{comp}(\alpha,\lambda',\mu',\kappa) - \delta\theta^{obse}\right)\end{array}\right\} \quad (17)$$

Where f and g are the functions used to measure the difference between the computed and observed quantity, in general we use the square function $f, g := \frac{1}{2}\|\cdot\|^2$.

$$\mathbf{S} = \lambda\mathrm{tr}(\mathbf{E})\mathbf{I} + 2\mu\mathbf{E} - (3\lambda+2\mu)\alpha(\theta-\theta_0)\mathbf{I} + \lambda'\mathrm{tr}(\dot{\mathbf{E}})\mathbf{I} + 2\mu'\dot{\mathbf{E}} \quad (18)$$

Definition 5.2 (Least square cost functions)**.** *For the first approximation, we define least square cost functions to identify the physical parameters of the model :*

$$\mathbf{x} = \inf_{\alpha\in\mathcal{R}_+}\inf_{\lambda'\in\mathcal{R}_+}\inf_{\mu'\in\mathcal{R}_+}\inf_{\kappa\in\mathcal{R}_+}\frac{1}{2}\left\{\begin{array}{l} \left\|\left(\frac{2}{J}\mathbf{F}\mathbf{S}\mathbf{F}^{\mathbf{T}}\right)^{comp}_{/33}(\alpha,\lambda',\mu') - \sigma^{obse}\right\|^2 \\ \left\|\delta\theta^{comp}(\alpha,\lambda',\mu',\kappa) - \left(\delta\theta^{obse}+273.15\right)\right\|^2\end{array}\right\} \quad (19)$$

5.2. Computation, splitting

We present in this section the computation setting using splitting methods. The main step is summarized by the following scheme.

1) **Define** : Initialization $[\alpha_0, \lambda'_0, \mu'_0, \kappa_0]$; $\quad \delta\theta_0 = \theta_0 + 273.15$, ν

2) **Minimize Self-heating model** :

•LOOP ($k = 0 \cdots n$)

---

a) **Minimize wave equation** : (input $[\alpha_k, \lambda'_k, \mu'_k, \kappa_k]$)

$$\mathbf{x} = \inf_{\alpha_k\in\mathcal{R}_+}\inf_{\lambda'_k\in\mathcal{R}_+}\inf_{\mu'_k\in\mathcal{R}_+}\inf_{\kappa_k\in\mathcal{R}_+}\frac{1}{2}\left\|\left(\frac{2}{J}\mathbf{F}\mathbf{S}\mathbf{F}^{\mathbf{T}}\right)^{comp}_{/33}(\alpha_k,\lambda'_k,\mu'_k) - \frac{F^{obs}(t)}{S^{\mathcal{B}}}\right\|^2$$

$$\textbf{if} \quad \frac{\lambda'_k}{2(\lambda'_k+\mu'_k)} \geq \nu \text{ (physical condition)}$$

LOOP wave equation ($k \longleftarrow k+1$)

else

End (output $[\alpha_k, \lambda'_k, \mu'_k, \kappa_k]$)

---

b) **Minimize heat equation** : (input $[\alpha_k, \lambda'_k, \mu'_k, \kappa_k]$)

$$\mathbf{x} = \inf_{\alpha_k \in \mathcal{R}_+} \inf_{\lambda'_k \in \mathcal{R}_+} \inf_{\mu'_k \in \mathcal{R}_+} \inf_{\kappa_k \in \mathcal{R}_+} \frac{1}{2} \left\| \delta\theta^{comp}\left(\alpha_k, \lambda'_k, \mu'_k, \kappa_k\right) - \left(\delta\theta^{obse} + 273.15\right) \right\|^2$$

$$\textbf{if} \quad |\alpha_k - \alpha_{k+1}, \lambda'_k - \lambda'_{k+1}, \mu'_k - \mu'_{k+1}, \kappa_k - \kappa_{k+1}| \geq \epsilon$$

•LOOP ($k \longleftarrow k+1$)
else
End (output $[\alpha_k, \lambda'_k, \mu'_k, \kappa_k]$)

Hypothesis 5.1 (Cost functions for one dimensional model)**.** *For the one dimensional model, the constant K_1 is known via λ, μ. The unknowns are K_2, K_3, K_4. We have to minimize the following cost function.*

$$\mathbf{x} = \inf_{K_2 \in \mathcal{R}_+} \inf_{K_3 \in \mathcal{R}_+} \inf_{K_4 \in \mathcal{R}_+} \frac{1}{2} \left\{ \begin{array}{l} \left\| (2\mathbf{S})^{comp}_{/33}\left(K_1, K_2\right) - \dfrac{F^{obs}(t)}{S^{\mathcal{B}}} \right\|^2, \\ \| \ \delta\theta^{comp}\left(K_1, K_2, K_3, K_4\right) - \left(\delta\theta^{obse} + 273.15\right) \ \|^2 \end{array} \right\} \tag{20}$$

6. Numerical approximations

In this section, we propose a finite element method for a 2D stess elasticity problem. The equations established in the previous section are solved using a finite elements discretization in space. In time, an implicit Euler scheme is applied for the time integration. In fact, we consider finite element approximations of the pure dynamic displacement traction/compression boundary value in three-dimensional nonlinear thermomechanical viscoelasticity associated with a homogenous viscoelastic material. We use the following weak form of the governing equation. The corresponding weak formulation in space-time is obtained by multiplying by the test functions : firstly, for the balance of momentum, by the scalar product with a vector-valued test function $\delta\mathbf{u}$ which has to be compatible with the geometric boundary conditions. Then, this equation is integrated over the volume of the sample.

$$\left\{ \begin{array}{l} \displaystyle\int_{\mathcal{B}} \mathbf{Div}\left[\rho(\lambda \mathrm{tr}(\mathbf{E})\mathbf{FI} + 2\mu\mathbf{FE}) - (3\lambda + 2\mu)\alpha\delta\theta\mathbf{FI}\right]\delta\mathbf{u}\, dV^{\mathcal{B}} \\ \displaystyle + \int_{\mathcal{B}} \mathbf{Div}\left[\lambda' \mathrm{tr}(\dot{\mathbf{E}})\mathbf{FI} + 2\mu'\mathbf{F}\dot{\mathbf{E}}\right]\delta\mathbf{u}\, dV^{\mathcal{B}} + \int_{\mathcal{B}} \rho\mathbf{B}\delta\mathbf{u}\, dV^{\mathcal{B}} = \int_{\mathcal{B}} \rho\frac{\partial\mathbf{v}}{\partial t}\delta\mathbf{u}\, dV^{\mathcal{B}} \\ \displaystyle\int_{\mathcal{B}} \rho c_v \frac{\partial\delta\theta}{\partial t}\delta\theta^*\, dV^{\mathcal{B}} = \int_{\mathcal{B}} (3\lambda + 2\mu)\alpha(\theta_0 + \delta\theta)\mathrm{tr}\dot{\mathbf{E}}\delta\theta^*\, dV^{\mathcal{B}} + \int_{\mathcal{B}} \lambda' \mathrm{tr}^2\dot{\mathbf{E}}\delta\theta^*\, dV^{\mathcal{B}} \\ \displaystyle + \int_{\mathcal{B}} 2\mu' \mathrm{tr}\dot{\mathbf{E}}^2\delta\theta^*\, dV^{\mathcal{B}} - \int_{\mathcal{B}} \kappa\theta_0\Delta\delta\theta\delta\theta^*\, dV^{\mathcal{B}} + \int_{\mathcal{B}} \rho r\delta\theta^*\, dV^{\mathcal{B}} \quad \forall\delta\theta^* \in [H^1(\mathcal{B})]^d \\ \mathbf{v} = \dfrac{\partial\mathbf{u}}{\partial t} \quad \text{in } (\mathcal{B} \times [0, T]) \end{array} \right. \tag{21}$$

For all $[\delta\Phi] = (\delta\mathbf{u}, \delta\theta^*)$. In which, $dV^{\mathcal{B}}$ and $dS^{\mathcal{B}}$ are respectively the volume and surface element. Using the divergence theorem and taking into account the boundary conditions,

the final representation of the weak form of the coupled self-heating model reads as follows :

$$\begin{cases} -\int_{\mathcal{B}} \rho(\lambda \mathrm{tr}(\mathbf{E})\mathbf{I} + 2\mu\mathbf{E}) : \nabla\delta\mathbf{u}^{\mathbf{T}}(\nabla\mathbf{u} + \mathbf{I})\, dV^{\mathcal{B}} - \int_{\mathcal{B}} (3\lambda + 2\mu)\rho\alpha\delta\theta\mathbf{I} : \nabla\delta\mathbf{u}^{\mathbf{T}} \\ (\nabla\mathbf{u} + \mathbf{I})\, dV^{\mathcal{B}} + \int_{\mathcal{B}} \left(\lambda' \mathrm{tr}(\dot{\mathbf{E}})\mathbf{I} + 2\mu'\dot{\mathbf{E}}\right) : \nabla\delta\mathbf{u}^{\mathbf{T}}(\nabla\mathbf{u} + \mathbf{I})\, dV^{\mathcal{B}} + \int_{\mathcal{B}} \rho\mathbf{B}\delta\mathbf{u}\, dV^{\mathcal{B}} \\ = \int_{\mathcal{B}} \rho\frac{\partial\mathbf{v}}{\partial t}\delta\mathbf{u}\, dV^{\mathcal{B}} \quad \forall\delta\mathbf{u} \in [H^1(\mathcal{B})]^d \\ \int_{\mathcal{B}} \rho c_v \frac{\partial\delta\theta}{\partial t}\delta\theta^*\, dV^{\mathcal{B}} = \int_{\mathcal{B}} (3\lambda + 2\mu)\alpha(\theta_0 + \delta\theta)\mathrm{tr}\dot{\mathbf{E}}\delta\theta^*\, dV^{\mathcal{B}} + \int_{\mathcal{B}} \lambda' \mathrm{tr}^2\dot{\mathbf{E}}\delta\theta^*\, dV^{\mathcal{B}} \\ + \int_{\mathcal{B}} 2\mu' \mathrm{tr}\dot{\mathbf{E}}^2\delta\theta^*\, dV^{\mathcal{B}} + \int_{\mathcal{B}} \kappa\theta_0\nabla\delta\theta.\nabla\delta\theta^*\, dV^{\mathcal{B}} - \int_{\partial\mathcal{B}} \kappa\theta\nabla\delta\theta.\mathbf{n}.\delta\theta^*\, dS^{\mathcal{B}} \\ + \int_{\mathcal{B}} \rho r\delta\theta^*\, dV^{\mathcal{B}} \quad \forall\delta\theta^* \in [H^1(\mathcal{B})]^d \\ \mathbf{v} = \dfrac{\partial\mathbf{u}}{\partial t} \quad \text{in } (\mathcal{B} \times [0, T]) \end{cases} \tag{22}$$

6.1. Computations

For the computation we use Comsol Multiphysics to compute the model by using general form of PDE. This tool allows us to solve systems of time-dependent or stationary partial differential equations in one, two, and three dimensions with complex geometry. There are two forms of the partial differential equations available, the general form and the coefficient form. They read

$$\begin{aligned} e_a\frac{\partial^2\mathbf{u}}{\partial t^2} + d_a\frac{\partial\mathbf{u}}{\partial t} + \nabla\cdot\Gamma = \mathbf{F} \text{ in } (\mathcal{B}\times[0,T]) \\ -\mathbf{n}\cdot\Gamma = G + \left(\frac{\partial R}{\partial\mathbf{u}}\right)^T\mu; 0 = R \text{ on } (\partial\mathcal{B}\times[0,T]) \end{aligned}$$

$$\begin{aligned} e_a\frac{\partial^2\mathbf{u}}{\partial t^2} + d_a\frac{\partial\mathbf{u}}{\partial t} + \nabla\cdot(-c\nabla\mathbf{u} - a\mathbf{u} + \gamma) + a\mathbf{u} + \beta\cdot\nabla\mathbf{u} = \mathbf{f} \text{ in } (\mathcal{B}\times[0,T]) \\ -\mathbf{n}(-c\nabla\mathbf{u} - a\mathbf{u} + \gamma) + q\mathbf{u} = g - h^T\mu; h\mathbf{u} = R \text{ on } (\partial\mathcal{B}\times[0,T]) \end{aligned} \tag{23}$$

respectively. The second kind of equation (coefficient form) can only be used for mildly nonlinear problems. For most nonlinear problems, the general form needs to be used.

Remark 6.1. *The coefficients of the coefficient form may depend both on x, t, and $\mathbf{u}$. Observe that a dependence on $\mathbf{u}$ is not recommended. The flux vector Γ and the scalar coefficient F, G and R can be function of the spatial coordinates the solution $\mathbf{u}$ and the space and time derivatives of $\mathbf{u}$. The variable μ is the Lagrange multiplier, and T denotes the transpose. q and g are respectively the boundary absorption coefficient and the boundary source term.*

The second method, to solve numerically the non-linear mechanics in this software is to define directly the thermodynamic potential in the software. The thermodynamic conditions as convexity must be verified before introducing the thermodynamic potential.

$$\nabla\cdot(\sigma^e + \sigma^v) + \rho\mathbf{b} = \rho\frac{\partial^2\mathbf{u}}{\partial t^2}; \quad \sigma^e = J^{-1}\mathbf{F}\mathbf{S}^{\mathbf{e}}\mathbf{F}^{\mathbf{T}} \quad \text{in } (\mathcal{B}\times[0,T])$$

$$\sigma^v = J^{-1}\mathbf{F}\mathbf{S}^{\mathbf{v}}\mathbf{F}^{\mathbf{T}} \quad \text{in } (\mathcal{B}\times[0,T]) \quad \mathbf{F} = \nabla\mathbf{u} + \mathbf{I}; \quad J = det\mathbf{F};$$
$$\mathbf{E} = (\mathbf{C}-\mathbf{I})/2; \quad \mathbf{C} = \mathbf{F}^{\mathbf{T}}\mathbf{F} = \mathbf{I} + \nabla\mathbf{u} + \nabla\mathbf{u} + \nabla^{\mathbf{T}}\mathbf{u}\nabla\mathbf{u}/2$$
$$\mathbf{S}^{\mathbf{e}} = 2\rho\frac{\partial\psi}{\partial\mathbf{C}}; \quad \mathbf{S}^{\mathbf{v}} = 2\frac{\partial\chi}{\partial\dot{\mathbf{C}}} \quad \text{in } (\mathcal{B}\times[0,T]) \tag{24}$$

In which, $\mathbf{F}$ is the deformation gradient, $\mathbf{I}$ is the identity matrix, $\mathbf{E}$ and $\mathbf{C}$ denote respectively the Green-Lagrange and the Cauchy-Green strain tensors. To solve numerically the self-heating model we assume : for the first approximation, we use the general form of PDE given by the equation (23) (first equation) for the wave and the heat equations. In a second approximation, we use the second method (24), it consists to introduce directly the thermodynamic potential for the wave equation and the general form of PDE for the heat equation. In this work, we use these methods to compare the numerical solution of the self-heating model.

$$\begin{bmatrix} e_a^{\mathbf{u}} & 0 \\ 0 & e_a^{\theta} \end{bmatrix}\frac{\partial^2}{\partial t^2}\begin{pmatrix}\mathbf{u}\\ \delta\theta\end{pmatrix} + \begin{bmatrix} d_a^{\mathbf{u}} & 0 \\ 0 & d_a^{\theta} \end{bmatrix}\frac{\partial}{\partial t}\begin{pmatrix}\mathbf{u}\\ \delta\theta\end{pmatrix} + \nabla\cdot\begin{bmatrix}\Gamma^{\mathbf{u}}\\ \Gamma^{\theta}\end{bmatrix} + \nabla\cdot\begin{bmatrix}\Gamma^{\dot{\mathbf{u}}}\\ \Gamma^{\dot{\theta}}\end{bmatrix}$$
$$= \begin{pmatrix}\mathbf{F}^{\mathbf{u}}\\ \mathbf{F}^{\theta}\end{pmatrix}$$
$$-\mathbf{n}\cdot(\Gamma^{\mathbf{u}} + \Gamma^{\dot{\mathbf{u}}}) = 0, \quad G = 0, \quad \text{on } (\Gamma_\ell\times[0,T])$$
$$\mathbf{R} = -\mathbf{u} \quad \text{on } (\Gamma_u\times[0,T])$$
$$\mathbf{R} = -\mathbf{u} - \mathbf{u}_0 \quad \text{on } (\Gamma_t\times[0,T])$$
$$-\mathbf{n}\cdot(\Gamma^{\theta} + \Gamma^{\dot{\theta}}) = 0, \quad G = 0, \quad \text{on } (\partial\mathcal{B} - \Gamma_c\times[0,T])$$
$$-\mathbf{n}\cdot\Gamma^{\theta} = h(\delta\theta - \delta\theta_{ref}), \quad G = 0, \quad \text{on } (\Gamma_c\times[0,T]) \tag{25}$$

Implementation in Comsol Multiphysics software is based on the equation 25.

6.2. Numerical approximations for local self-heating

Using the hypothesis for local self-heating in the sample, (Cf. hypothesis 3.2). The equation (**??**) becomes :

$$\begin{bmatrix} \rho & 0 \\ 0 & 0 \end{bmatrix}\frac{\partial^2}{\partial t^2}\begin{pmatrix}\mathbf{u}\\ \delta\theta\end{pmatrix} + \begin{bmatrix} 0 & 0 \\ 0 & \rho c_v \end{bmatrix}\frac{\partial}{\partial t}\begin{pmatrix}\mathbf{u}\\ \delta\theta\end{pmatrix} + \nabla\cdot\begin{bmatrix}\mathbf{F}\mathbf{S}^{\mathbf{e}}\\ 0\end{bmatrix}$$
$$+\nabla\cdot\begin{bmatrix}\mathbf{F}\mathbf{S}^{\mathbf{v}}\\ 0\end{bmatrix} = \rho\begin{pmatrix}\mathbf{B}\\ r\end{pmatrix} \tag{26}$$

In which

$$\mathbf{B} = 0; \qquad r = (3\lambda+2\mu)\alpha(\theta_0+\delta\theta)\mathrm{tr}\dot{\mathbf{E}} + \lambda'\mathrm{tr}^2\dot{\mathbf{E}} + 2\mu'\mathrm{tr}\dot{\mathbf{E}}^2$$
$$\mathbf{S}^{\mathbf{e}} = \lambda\mathrm{tr}(\mathbf{E})\mathbf{I} + 2\mu\mathbf{E} - (3\lambda+2\mu)\alpha(\theta-\theta_0)\mathbf{I}; \qquad \mathbf{S}^{\mathbf{v}} = \lambda'\mathrm{tr}(\dot{\mathbf{E}})\mathbf{I} + 2\mu'\dot{\mathbf{E}} \tag{27}$$

Implementation in Comsol Multiphysics software is based on the equation (26).

6.3. Numerical approximations for non-local self-heating

Cf. hypothesis 3.3. The equation (25) becomes :

$$\begin{bmatrix} \rho & 0 \\ 0 & 0 \end{bmatrix}\frac{\partial^2}{\partial t^2}\begin{pmatrix}\mathbf{u}\\ \delta\theta\end{pmatrix} + \begin{bmatrix} 0 & 0 \\ 0 & \rho c_v \end{bmatrix}\frac{\partial}{\partial t}\begin{pmatrix}\mathbf{u}\\ \delta\theta\end{pmatrix} + \nabla\cdot\begin{bmatrix}\mathbf{F}\mathbf{S}^{\mathbf{e}}\\ \kappa\nabla\delta\theta\end{bmatrix}$$
$$+\nabla\cdot\begin{bmatrix}\mathbf{F}\mathbf{S}^{\mathbf{v}}\\ 0\end{bmatrix} = \rho\begin{pmatrix}\mathbf{B}\\ r\end{pmatrix} \tag{28}$$

in which

$$\mathbf{B} = 0; \qquad r = (3\lambda + 2\mu)\alpha(\theta_0 + \delta\theta)\mathrm{tr}\dot{\mathbf{E}} + \lambda'\mathrm{tr}^2\dot{\mathbf{E}} + 2\mu'\mathrm{tr}\dot{\mathbf{E}}^2$$
$$\mathbf{S^e} = \lambda\mathrm{tr}(\mathbf{E})\mathbf{I} + 2\mu\mathbf{E}; \qquad \mathbf{S^v} = \lambda'\mathrm{tr}(\dot{\mathbf{E}})\mathbf{I} + 2\mu'\dot{\mathbf{E}} \tag{29}$$

Implementation in comsol multiphysics software is based on the equation (28).

7. Experimental and numerical results

As a first result, we want to verify that the experimental measurement of the temperature in the sample is not biaised by the friction between the hydrogel and the temperature sensor in the microcalorimeter during the deformation. We can then conclude that there is no temperature increase due to the friction and, then, eventual temperature increase will be due to self-heating phenomenon of the tested sample. The effect of the self-heating and corresponding temperature increase in the hydrogel is presented in figure 2. A clear

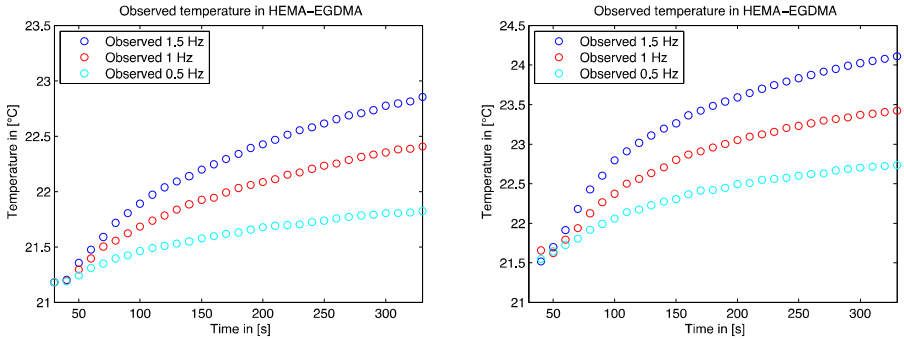

Figure 2. *Observed temperature in the sample of HEMA-EGDMA vs. time for* $\phi = 6\%$ *(left) and* $\phi = 8\%$ *(right),* $f = 0.5$ *[Hz],* $f = 1$ *[Hz] and* $f = 1.5$ *[Hz].*

temperature increase is obtained over time for the three different frequencies and two different cross-linkers concentration. The temperature increases between the initial and last cycles read 2.5^oC. There is clear dependency of the temperature increase to the applied frequency. The higher the frequency is, the higher the temperature increases. These experimental temperature evolution were used to identify the parameters present in the analytical 1D model. A good correlation is obtained between the experimental data and the model as shown in figure 3.

Based on the these correlations, the obtained identified parameters of the model are reported in Table 1.

Samples	$\lambda'[MPa.s]$	$\mu'[MPa.s]$	$\alpha[1/K]$
Sample 1	357.93	39.77	1.9e-4
Sample 2	393.646	51.701	2.1e-4

Tableau 1. *Optimized constants of the samples after equation* (20)

Finally the parameters reported on table 1 were injected in the FEM model (see equation (21)) and the computed temperature evolutions were then plotted in figure 4 It can

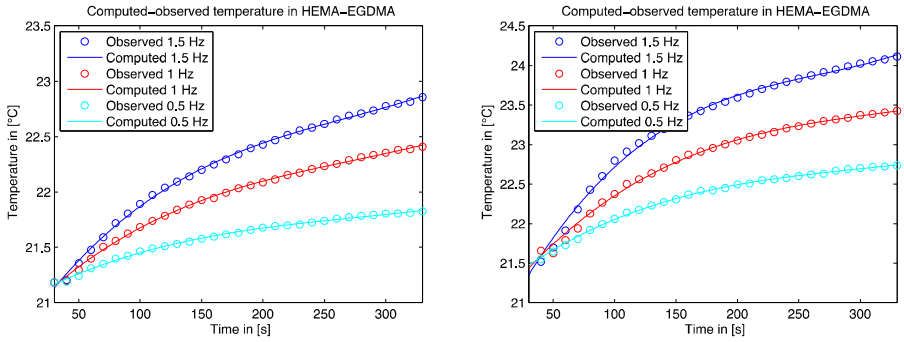

Figure 3. *Correlation between computed (analytical solution) and observed temperature in the sample of HEMA-EGDMA vs. time. for* $\phi = 6\%$ *(left) and* $\phi = 8\%$ *(right),* $f = 0.5$ *[Hz],* $f = 1$ *[Hz] and* $f = 1.5$ *[Hz].*

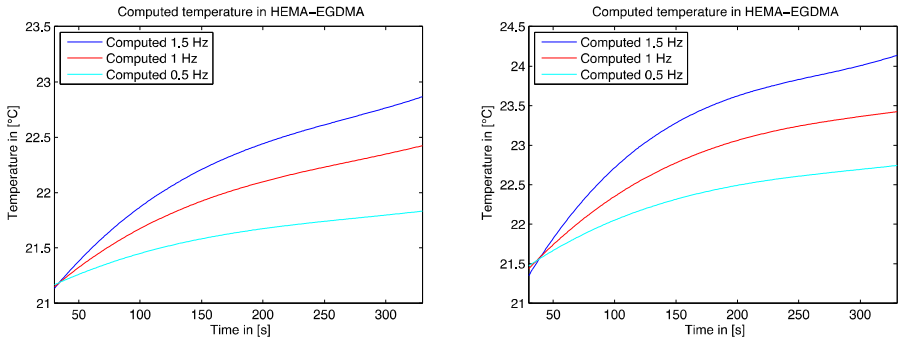

Figure 4. *Computed (numerical model) temperature in the sample of HEMA-EGDMA vs. time for* $\phi = 6\%$ *(left) and* $\phi = 8\%$ *(right),* $f = 0.5$ *[Hz],* $f = 1$ *[Hz] and* $f = 1.5$ *[Hz].*

be obtained that the obtained curves closely match the experimental measurement of the hydrogel self-heating, not only the frequency dependence, but also the cross-linkers dependence could be caught by the developed model.

7.1. Influence of the cross-link density on the self-heating

In order to have a closer look to the influence of cross-link density on the self-heating, we report on the same graph the temperature evolution of the hydrogels for the two different cross-linker density (6% and 8%). It can be observed on figure 5 that the decrease in the cross-linker density caused a significant change in the heat production and consequently a more limited temperature increase during cyclic loading. The effect of the cross-link density is implicitly taken into account in the model through the dependency of the cross-link density in the model parameters.

7.2. Dissipation in function of frequency and cross-link density

In this subsection, we present the experimental results for the dissipation in the hydrogel obtained from the force-displacement hysteresis curves. We evaluate the effect of the temperature increase on the dissipation during the different phase of the test (preloading, cyclic loading and relaxation).

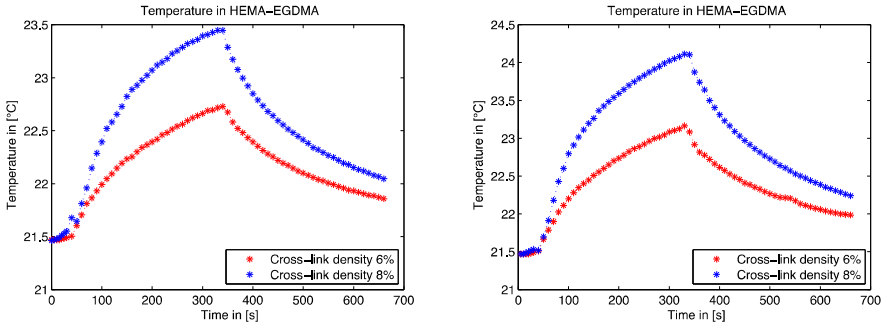

Figure 5. *Temperature (in [°C]) vs. time (in [s]) in the HEMA-EGDMA samples. The curves show the effect of the cross-link density ϕ on the temperature during test (preloading, cyclic loading and relaxation). $f = 1$ [Hz] for the cyclic loading.*

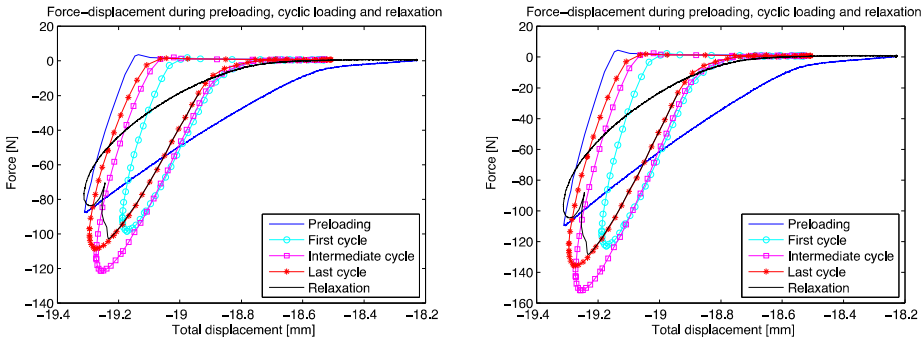

Figure 6. *Hysteresis cycle. The curves represent the response of the sample, force in function of the total displacement (during the test, preloading, cyclic loading 5 [mn] and relaxation). $\phi = 6\%$, $f = 0.5$ [Hz] (left) and $f = 1$ [Hz] (right).*

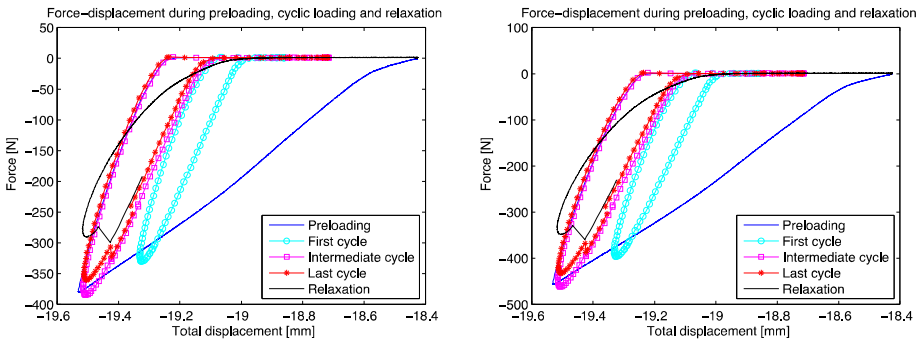

Figure 7. *Hysteresis cycle. The curves represent the response of the sample, force in function of the total displacement (during the test, preloading, cyclic loading 5 [mn] and relaxation). $\phi = 8\%$, for $f = 0.5$ [Hz] (left) and $f = 1$ [Hz] (right).*

We also illustrate the variation of the hydrogel dissipation in function of the cross-link density and the frequency. Without surprise, it can be seen in figures 6 and 7 that

the dissipation is function of the cross-link density and the frequency of loading as for the temperature evolution. More interestingly, we can also observe from this figure that the shape of the hysteresis curves depends on the number of loading cycles. For the same sample under the same loading condition, the shape of the hysteresis curves is completely different if we consider the first, the intermediate or the last cycles. As there is a direct correspondence between the number of cycles and the corresponding temperature in the sample (through the temperature evolution presented in figure 2 (for example), we can deduce that the dissipation is then also function of the temperature.

Indeed, a closer look to the Figures 6 and 7 highlights that the behavior of the hydrogel presents a shift between elastic, viscoelastic and again elastic behaviors at two critical temperatures. This unexpected (and to the best of our knowledge not reported before) behavior was observed for all tested samples.

8. Concluding remarks

In this paper a combined analytical-numerical-experimental approach was developed to evaluate the self-heating phenomenon in a specific hydrogel. The proposed methods are general enough to be used to characterize other types of materials. We demonstrate in this study that the developed model could adequately describe the self-heating behavior of the hydrogel. The influence of two main parameters (cross-link density and loading frequency) on the temperature evolution could also be taken into account in the model. We have to mention that the ranges of the frequency in this work were limited to 0.1-2 Hz for the numerical approaches and to 0.5-1.5 Hz for the experimental measurements. The cross-link density of the hydrogel was limited to 6% and 8% and the percentage in water is prescribed to 40%.

From the experimental data, it has been observed that the hysteresis characterizing the dissipation through the loop force-displacement during the harmonic loading changes its shape in function of the cycle numbers. Two phenomena could be taken into account to explain this observation. First, we can consider that during the loading, the internal structure of the hydrogel changes adapting its structure to the loading. The second phenomenon, which could explain the change of the hysteresis curve over time, is the change in temperature of the self-heating hydrogel. As the number of cycles increases so do the hydrogel temperature. It can then be considered that the increase of temperature changes the mechanical parameters of the hydrogel. For example, in the situation where the elastic parameters would increase with the temperature, as the same displacement was experimentally imposed on the hydrogel, an increase mechanical energy will then be transmitted to the hydrogel.

In general, the developed model could be useful in the phase of design of the hydrogel for a particular application. For example, with the idea of using this kind of dissipative hydrogel for the controlled delivery of a drug through the temperature increase , a link has to be established between the number of cycles and the targeted temperature increase. The developed model would then be useful in this situation to determine the cross-link density needed and/or the mechanical loading regime that the hydrogel should be exposed to. In another application, it has been shown that the toughness of the hydrogel could be increased by increasing its dissipative properties . Again in this situation, the developed model could be used to design the most dissipative hydrogel under known mechanical conditions.

Acknowledgment

Financial supports by the International Doctoral College (CDI) of the Brittany European University (UEB), the Brittany Region Council (France) and the Laboratory of Biomechanical Orthopedics (Lausanne, Switzerland) are greatly appreciated.

9. Bibliographie

[1] A.M. LOWMAN, N.A. PEPPAS, « Hydrogels,Encyclopedia of Drug Delivery », *John Wiley& Sons*, 1999.

[2] N.A. PEPPAS, « Hydrogels in medicine », *Boca Raton, CRC Press*, 1987.

[3] A.S. HOFFMAN , « Hydrogels for biomedical applications, », *Advanced Drug Delivery Reviews*, n° 60, 2002.

[4] M. NASSAJIAN MOGHADAM, V. KASELOV, A. VOGEL, H-A. KLOK « Controlled release from a mechanically-stimulated thermosensitive self-heating composite hydrogel, », *Biomaterials*, n° 35, 2014.

[5] P. ABDEL-SAYED, M. NASSAJIAN MOGHADAM, R. SALOMIR, D. TCHERNIN, D. PIOLETTI « Intrinsic viscoelasticity increases temperatures in knee cartilage under physiological loading, », *Journal of the mechanical behaviour of biomedical materials*, n° 30, 2014.

[6] L. RAKOTOMANANA, D. PIOLETTI, « Non-linear viscoelastic laws for soft biological tissues », *Eur. J. A/Solids*, n° 19, 2000.

[7] TRUESDELL, COLLEMAN, NOLL « The non-linear theories of mechanics », *Springer*, 1992.

[8] M. NASSAJIAN MOGHADAM, D. PIOLETTI, « Improving hydrogels toughness by increasing the dissipative properties of their network », *J Mech Behav. Biomed. Mat.*, n° 41, 2015.

[9] L. RAKOTOMANANA, « Elément de dynamique des solides et structures déformables », *Presses Polytechniques et Universitaires Romandes*, 2009.

[10] R. ZHENG, P. KENNEDY, N. PHAN-THIEN, X-J. FAN, « Thermoviscoelastic simulation of thermally and pressure-induced stresses in injection moulding for the prediction of shrinkage and warpage for fiber-renforced thermoplastics », *Journal of Non-Newtonian Fluid Mechanics*, n° 84, 1999.

[11] C. MORIN, Z. MOUMNI, W. ZAKI « Thermomechanical coupling in shape memory alloys under cyclic loadings : Experimental analysis and consitutive modeling », *Journal maths pures Applied*, n° 27 2011.

[12] N. SANTATRINIAINA, J. DESEURE, T.Q. NGUYEN, T.Q. NGUYEN, H. FONTAINE, C. BEITIA, L. RAKOTOMANANA « Coupled system of PDEs to predict the sensitivity of some materials constituents of FOUP with the AMCs cross–contamination », *International Journal of Applied Mathematical Research*, n° 3 2014.

[13] N. SANTATRINIAINA, J. DESEURE, T.Q. NGUYEN, T.Q. NGUYEN, H. FONTAINE, C. BEITIA, L. RAKOTOMANANA « Mathematical modeling of the AMCs cross–contamination removal in the FOUPs : Finite element formulation and application in the FOUP's decontamination », *International Journal of Mathematical, Computational Science Engineering*, n° 8 2014.

[14] K. KUNISCH , G. LEUGERING , G. LEUGERING , J.SPREKELS , T. FREDI « Optimal Control of the Coupled Systems of Partial Differential Equations », *International Series of Numerical Mathematics*, n° 158, 2009.